

Microscopic evidence for Fulde-Ferrel-Larkin-Ovchinnikov state and multiband effects in KFe_2As_2 X. Y. Liu^{1,2}, Z. Kao³, J. Luo¹, J. Yang¹, A. F. Fang^{4,5}, J. Zhao^{3,6,7}, R. Zhou^{1,*}, and Guo-qing Zheng⁸¹*Institute of Physics, Chinese Academy of Sciences, and Beijing National Laboratory for Condensed Matter Physics, Beijing 100190, China*²*School of Physical Sciences, University of Chinese Academy of Sciences, Beijing 100190, China*³*State Key Laboratory of Surface Physics and Department of Physics, Fudan University, Shanghai, China*⁴*School of Physics and Astronomy, Beijing Normal University, Beijing 100875, China*⁵*Key Laboratory of Multiscale Spin Physics, Ministry of Education, Beijing Normal University, Beijing 100875, China*⁶*Shanghai Research Center for Quantum Sciences, Shanghai, China*⁷*Institute of Nanoelectronics and Quantum Computing, Fudan University, Shanghai, China*⁸*Department of Physics, Okayama University, Okayama 700-8530, Japan*

(Received 4 December 2024; revised 2 June 2025; accepted 30 June 2025; published 17 July 2025)

The Fulde-Ferrell-Larkin-Ovchinnikov (FFLO) state is a superconducting phase characterized by broken translational symmetry, where Cooper pairs form with nonzero momentum between Zeeman-split Fermi surfaces. This state is highly sensitive to band structure and pairing symmetry. In multiband superconductors, the FFLO state can significantly deviate from its standard form, but experimental verification has remained challenging. Here, we present ⁷⁵As nuclear magnetic resonance (NMR) measurements on the multiband superconductor KFe_2As_2 . In the low-temperature, high-magnetic-field region above the upper critical field B_{c2} , we observe a clear increase in the second moment of the NMR spectrum, along with a strong enhancement in the spin-lattice relaxation rate divided by temperature $1/T_1T$. These results indicate an emergence of superconducting spin smecticity and Andreev bound states from the spatial modulation of the superconducting gap, providing microscopic evidence for the FFLO state. The obtained phase diagram reveals a distinct boundary line between the FFLO and homogenous superconducting states with a low critical temperature of the FFLO state $T^* \approx 0.2T_c$, which can be attributed to the multiband effects in KFe_2As_2 . Our results show that the iron-based superconductors are a good material platform for studying the FFLO state and highlight the importance of the multiband effects on this exotic phase.

DOI: [10.1103/PhysRevB.112.L020505](https://doi.org/10.1103/PhysRevB.112.L020505)

Introduction. As the external magnetic field approaches the Pauli limit field B_{Pauli} , the conventional superconducting (SC) state becomes metastable, giving way to a new superconducting state with spontaneous translational-symmetry breaking, which is known as the Fulde-Ferrell-Larkin-Ovchinnikov (FFLO) state [1–5], where Cooper pairs are formed with electrons from two Zeeman-split Fermi surfaces. Consequently, these pairs have a nonzero center-of-mass momentum, resulting in a spatially modulated energy gap, a defining feature that distinguishes the FFLO state from other unconventional SC states. Despite theoretical predictions of rich physical phenomena in the FFLO state, direct experimental observation has been challenging. The FFLO candidates should have a sufficiently large Maki parameter, $\alpha_M = \sqrt{2}B_{\text{orb}}(0)/B_{\text{Pauli}}(0) > 1.8$, which is a measure of the paramagnetic pair-breaking strength [6]. Besides this, the appearance of the FFLO state also requires an extremely small number of disorders in the sample, as the impurity scattering suppresses its formation [7]. Previous studies using bulk measurements such as the magnetostriction, ultrasound velocity, and heat capacity have reported an upturn of the upper critical field and a transition inside the superconducting phase in heavy

fermion superconductors [8], low-dimensional organic superconductors [9,10], and transition metal dichalcogenide superconductors [11,12]. Iron-based superconductors, known for their quasi-two-dimensional structure, strong Pauli paramagnetic effect, and multiband nature, are considered an ideal platform for investigating FFLO physics [13,14]. Previous transport and specific heat measurements have suggested the potential presence of an FFLO state in FeSe above the upper critical field B_{c2} [15,16]. However, the observed high-field superconducting states were found to be insensitive to disorders, which is inconsistent with the characteristics of the FFLO state [17]. Notably, there is currently no microscopic experimental evidence supporting the existence of the FFLO state in iron-based superconductors.

Nuclear magnetic resonance (NMR) can serve as a powerful tool for investigating the FFLO state in bulk superconductors, directly detecting the superconducting spin smecticity, a property in analogy with liquid crystal, arising from the staggered distribution of normal and superconducting regions, resulting in line splitting or broadening in the spectrum [18]. Furthermore, nodes in the order parameter form domain walls due to this staggered distribution, leading to a phase twist of π in the superconducting phase and local modification of electronic density of states, creating Andreev bound states [19,20]. The polarized quasiparticles spatially

*Contact author: rzhou@iphy.ac.cn

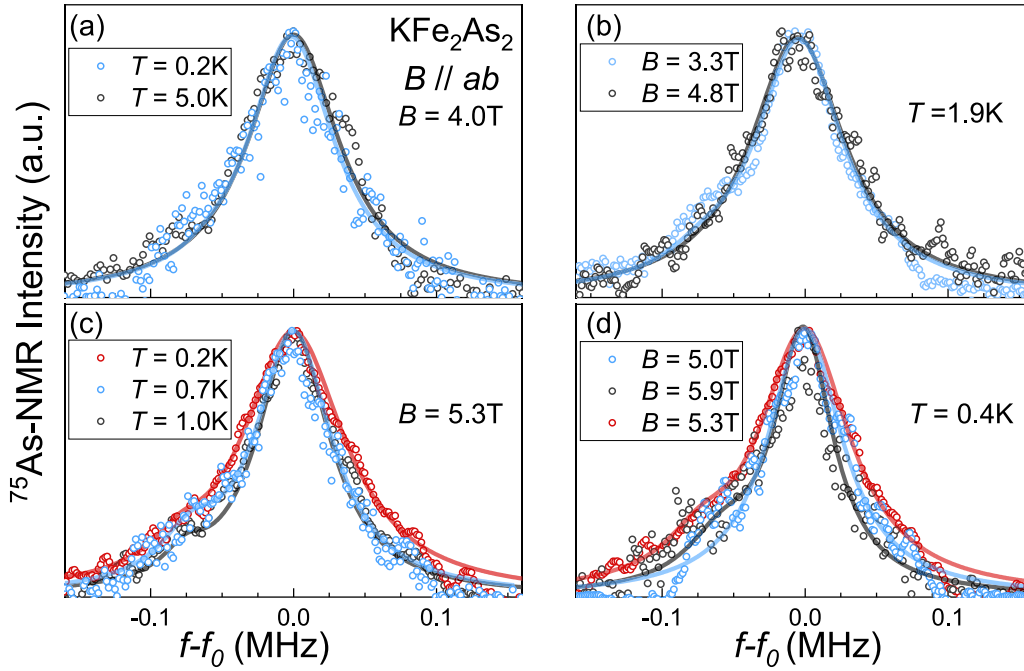


FIG. 1. (a)–(d) Central line of ^{75}As -NMR spectra in the normal state (black color), the homogeneous superconducting state (blue color), and the FFLO state (red color) with the external magnetic field applied along the ab plane (see the Supplemental Material for all spectra at various temperatures and fields [42]). f_0 (~ 24 – 45 MHz) is the frequency of the center of the shown spectra. Solid lines are guides to the eye.

localized in the nodes can enhance the spin-lattice relaxation rate divided by temperature $1/T_1 T$ [21]. However, these two behaviors have not been simultaneously observed in one single superconducting material. For instance, previous studies on CeCoIn_5 [22,23], $\beta''\text{-(ET)}_2\text{SF}_5\text{CH}_2\text{CF}_2\text{SO}_3$ [24], and Sr_2RuO_4 [25] only reported line splitting or broadening without any anomaly in $1/T_1 T$, while no NMR line anomaly was reported in $\kappa\text{-(BEDT-TTF)}_2\text{Cu(NCS)}_2$ [21] and CeCu_2Si_2 [26]. Therefore, further experimental measurements remain essential to verify the existence of the FFLO state in general and especially for investigating multiband effects in the emergent materials.

KFe_2As_2 is particularly clean compared to other iron-based superconductors. The residual resistivity ratio of this compound can be even up to 3000 [27]. Experiments have shown that the upper critical field B_{c2} of KFe_2As_2 is decided by the Pauli paramagnetic effect with Maki parameter $\alpha_M \sim 3$ [28,29]. Additionally, its anisotropic Fermi surface and superconducting order parameter together favor the formation of FFLO Cooper pairs [30–33]. Previous magnetic torque and specific heat measurements have indeed observed the upturn of the upper critical field at low temperatures and high fields in KFe_2As_2 [34]. However, these findings do not explicitly address the multiband effect on the FFLO state. Such effect can broaden the parameter space where FFLO states can form and affect boundaries between FFLO and homogenous superconducting (HSC) states [35–39]. Therefore, direct microscopic experimental investigations are required for the putative state and for establishing a precise FFLO boundary in KFe_2As_2 .

Methods. In this work, we use ^{75}As -NMR to address these issues. We found microscopic evidence for a FFLO state both from NMR spectra and $1/T_1 T$. We established a concrete boundary between the FFLO and homogeneous

superconducting states, which is different from what is expected for a single-band superconductor. The single crystal samples were grown by the self-flux method that is described in Refs. [40,41]. The superconducting critical temperature T_c of our sample is 3.8 K from the ac susceptibility measurement [42], which is among the highest reported for this compound, indicating its high quality [27]. Below $T = 1.5$ K, measurements were conducted by using a ^3He - ^4He dilution refrigerator. To minimize the heating effects at low temperatures, we used a 30- μs -long $\pi/2$ pulse. We adopt the same method as that of Pustogow *et al.* [43] to test the heat-up effect induced by rf pulses in the superconducting state. We also confirmed that the spin-lattice relaxation rate $1/T_1$ is nearly frequency independent. Subsequently, all T_1 was measured at the central position of the NMR line. Further details can be found in Figs. S3 and S12(a) [42]. The external magnetic field was applied parallel to the ab plane with precise angle control achieved through a single axis rotator (see Supplemental Material [42] Fig. S5). The NMR spectra were obtained by summing the fast Fourier transforms of the spin-echo signals, while the spin-lattice relaxation rate $1/T_1$ was measured by the saturation-recovery method. Field values were calibrated using the resonance frequency of ^{63}Cu in the copper coil ($^{63}\text{K} = 0.235\%$ at low temperatures).

NMR results. Figure 1 presents the central transition line of the ^{75}As -NMR spectra at various temperature and magnetic fields. No spectral changes are observed with temperature down to 0.2 K at $B = 4$ T nor with any magnetic fields at $T = 1.9$ K [Figs. 1(a) and 1(b)]. However, at $B = 5.3$ T, line broadening appears at low temperatures below 0.6 K [Fig. 1(c)]. At $T = 0.4$ K, line broadening appears within a small field region $5 \text{ T} < B < 5.9 \text{ T}$ [Fig. 1(d)]. To quantify this broadening, we calculate the square root of the second moment

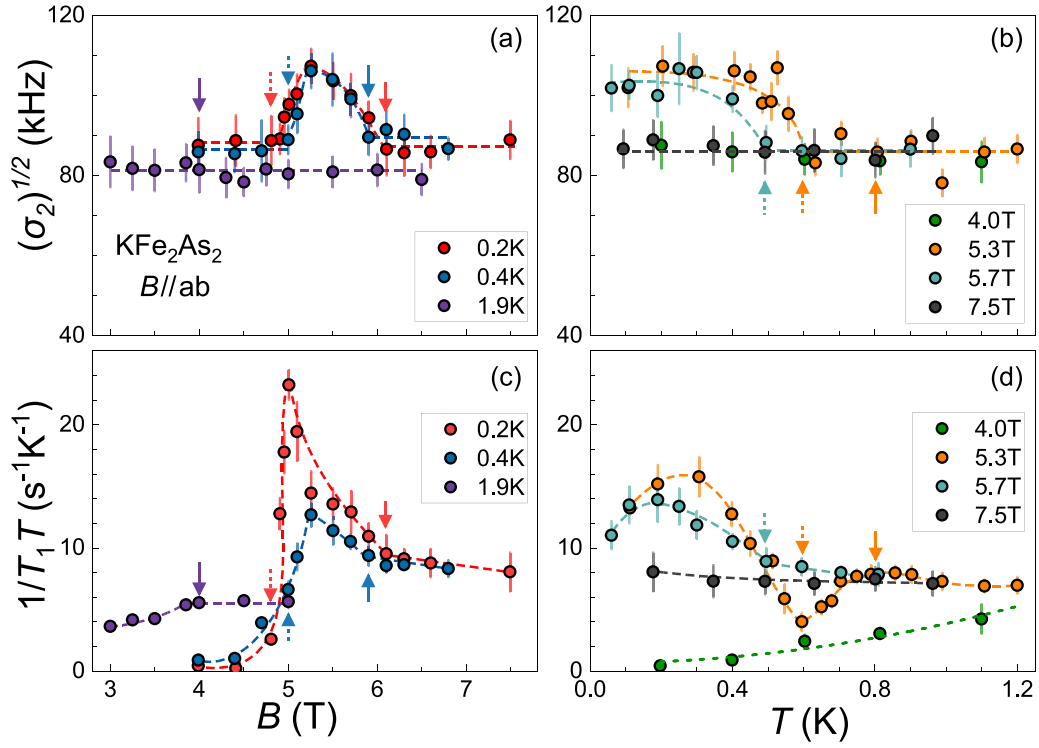


FIG. 2. Panels (a) and (c) are the field dependence of $(\sigma_2)^{1/2}$ of the spectrum and $1/T_1T$ at various temperatures, respectively. Panels (b) and (d) are the temperature dependence of the second moment of the spectra $(\sigma_2)^{1/2}$ and $1/T_1T$ at various fields, respectively. The solid arrows denote a transition from the normal state to the HSC state. The dashed arrows identify a transition from the normal state or the HSC state to the FFLO state. Dashed lines are guides to the eye.

of the spectra $(\sigma_2)^{1/2}$ [42], which is a sensitive indicator of spin polarization [25,26,44]. The results of the calculation are presented in Figs. 2(a) and 2(b), revealing a clear line broadening at low temperatures and high magnetic fields, at $T = 0.2$ K with $4.8 \text{ T} < B < 6.1 \text{ T}$, $T = 0.4$ K with $5 \text{ T} < B < 5.9 \text{ T}$, $T < 0.6$ K at $B = 5.3 \text{ T}$, and $T < 0.5$ K at $B = 5.7 \text{ T}$. In these regions, although no decrease in Knight shift was observed due to the broad central lines [42], ac susceptibility measurements indicate that the NMR line broadening indeed takes place within the superconducting state, even when the magnetic field exceeds the Pauli limit field $B_{\text{Pauli}} = 4.8 \text{ T}$ [34]. When an external field is applied parallel to the superconducting layers of KFe_2As_2 , the Josephson vortex state forms only between these layers and should not affect the linewidth, consistent with the temperature-independent behavior of $(\sigma_2)^{1/2}$ at $B = 4 \text{ T}$ in the superconducting state [see Fig. 2(b)]. The enhancement of $(\sigma_2)^{1/2}$ of the spectrum occurs only within a magnetic field range of $4.8 \text{ T} < B < 6.1 \text{ T}$ and below $T \approx 0.8 \text{ K}$, suggesting that the emergent line broadening is unrelated to the vortex state. Instead, it arises from the superconducting spin smecticity, which is a characteristic feature of the FFLO state, as we elaborate below. In principle, the line splitting with a two-horn structure, as observed in Sr_2RuO_4 [25], should be present [see Fig. S8(a)] [42]. However, in KFe_2As_2 , only line broadening is observed due to the relatively larger linewidth of the central line due to the second-order quadrupolar broadening [see Figs. S8(b) and S8(c)] [42]. We thus define the critical temperature T^* or magnetic field B^* of this possible FFLO state as the point at which the $(\sigma_2)^{1/2}$ of the spectrum begins to increase.

To gain further insight into the inhomogeneous superconducting state, we measured the $1/T_1T$ as shown in Figs. 2(c) and 2(d). At $B = 4 \text{ T}$, the temperature dependence of $1/T_1$ exhibits a rapid decrease with a T^3 variation at low temperatures, with no Hebel-Slichter coherence peak [42], suggesting the unconventional nature of the superconductivity. The $1/T_1 \propto T^3$ behavior is in contrast to other iron-based superconductors [45,46], but is consistent with the existence of line nodes in the gap function as previously observed by the angle-resolved photoemission spectroscopy (ARPES) [30,33]. A rapid reduction in $1/T_1T$ is also observed below the upper critical field $B_{c2} = 4 \text{ T}$ at $T = 1.9 \text{ K}$ [see Fig. 2(c)]. As the magnetic field increases, distinct peaks in $1/T_1T$ are observed at 5.3 T and 5.7 T , coinciding with the temperatures at which $(\sigma_2)^{1/2}$ of the NMR spectrum begins to increase. Additionally, at $T = 0.2 \text{ K}$ and 0.4 K , peaks are also observed in the field variation of $1/T_1T$, at the magnetic fields where $(\sigma_2)^{1/2}$ increases [see Fig. 2(c)]. The correlation between the second moment $(\sigma_2)^{1/2}$ and the $1/T_1T$ indicates that the emergence of the superconducting spin smecticity and Andreev bound states occurs within the same temperature and high-field region. Our results provide compelling evidence for the existence of the FFLO state. Notably, at 5.3 T , there is a decrease in the $1/T_1T$ values in range $T^* < T < T_c$, suggesting that the sample first transitions into the HSC state before evolving into the FFLO state as the temperature decreases. In the FFLO state, one would also anticipate that $1/T_1T$ could be frequency dependent due to the spin smecticity. We indeed observed a frequency dependence of $1/T_1T$ [see Fig. S12(b)], although rather weak. Nevertheless, the disparity of $1/T_1T$ between the lowest and

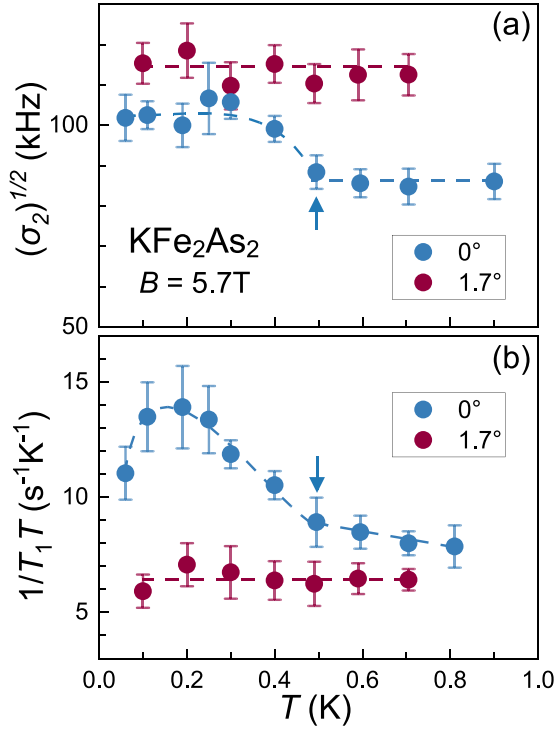


FIG. 3. Comparison of the temperature dependence of $(\sigma_2)^{1/2}$ and $1/T_1T$ between $\theta = 0^\circ$ (blue color) and 1.7° (red color) at $B_0 = 5.7$ T in KFe_2As_2 . The solid arrows represent a transition from the normal state to the FFLO state. Dashed lines are guides to the eye.

highest frequency points was within the error margin. The frequency-dependent behavior of $1/T_1T$ could be smeared out in KFe_2As_2 , as the NMR spectra merely exhibit line broadening, instead of the line splitting observed in Sr_2RuO_4 [25]. It would be interesting to conduct similar measurements on Sr_2RuO_4 in the FFLO state in the future. At $B = 7.5$ T, the $1/T_1T$ data show a slight upturn as the temperature decreases, which can be attributed to spin fluctuations [47].

For a FFLO state in quasi-two-dimensional superconductors, it should be sensitive to the field orientation [48]. The FFLO state can be significantly suppressed when the magnetic field deviates from being parallel to the superconducting layers, leading to the competition with the Abrikosov vortex state that forms within the superconducting layer. Upon rotating the sample by 1.7° , we indeed found that $(\sigma_2)^{1/2}$ of the spectra becomes temperature independent and the peak in $1/T_1T$ disappears, as shown in Figs. 3(a) and 3(b), respectively. These results show that the observed high-field state is indeed highly sensitive to the angle between the external field and the ab plane, consistent with previous specific heat measurements [34].

Phase diagram and discussions. We summarize our experimental findings in the phase diagram presented in Fig. 4. Comments on two characteristic features found in this study are in order. First, the transition field from HSC to FFLO state decreases as temperature decreases. The decreasing transition field from HSC to FFLO state with decreasing temperature suggests that the FFLO state may be more readily formed at lower temperatures. We ascribe this phenomenon to interband

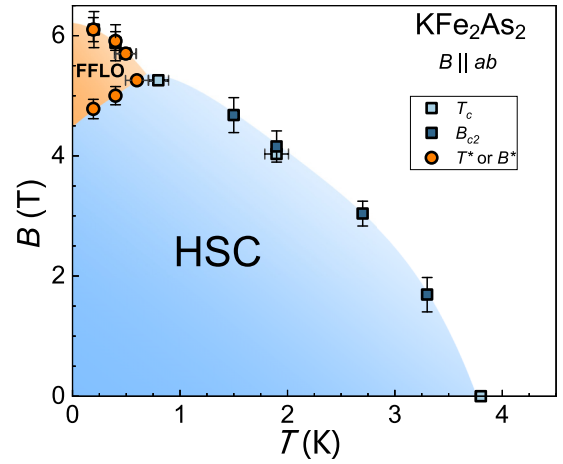


FIG. 4. Obtained phase diagram. The light blue and dark blue squares represent the superconducting critical temperature T_c and the upper critical field B_{c2} obtained from the ac susceptibility measurements [42]. The orange circle is the onset field B^* and temperature T^* determined based on the increase of $(\sigma_2)^{1/2}$ and $1/T_1T$. HSC and FFLO denote the homogeneous superconducting state and the Fulde-Ferrell-Larkin-Ovchinnikov state, respectively.

coupling in KFe_2As_2 as elaborated below. Because of the finite center-of-mass momenta of the Cooper pairs, the stability of the FFLO state strongly depends on the Fermi surface structure and the pairing anisotropy [36]. Recent ARPES studies have demonstrated the presence of multiple Fermi surfaces with different anisotropies in KFe_2As_2 [33]. The α and γ Fermi surface is nearly isotropic. The superconducting gap on the α Fermi surface is also nearly isotropic and it is nearly zero on the γ Fermi surface. In contrast, the β and ε Fermi surfaces display anisotropy, with a line-nodal superconducting gap which can facilitate the FFLO formation. Additionally, ARPES measurements also suggested that the normal state of the ε band features a very flat band, which can enhance the stabilization of the FFLO state through nesting [9,38]. Therefore, the observed FFLO pairing in KFe_2As_2 can be mainly ascribed to the two anisotropic Fermi surfaces. Now, previous numerical calculations have shown that the FFLO state can be stabilized even in the lower field region due to interband coupling between an active band and a passive band where a gap is negligibly small [36]. In the present case, the superconducting gap in the γ band is much smaller than that in the other bands [33], so that the theory of Ref. [36] can apply. Namely, coupling between the γ and other bands can result in a decrease in the lower critical field of the FFLO state at low temperatures and establishes an ascending boundary line between the FFLO state and HSC state as observed in the phase diagram of KFe_2As_2 .

Secondly, we found a low critical temperature $T^* \approx 0.2T_c$ of the FFLO state. For the heavy fermion and organic superconductors, the T^*/T_c ratio is larger than 0.4 in possible FFLO states [8–10], where the Maki parameter is typically very large, implying that the orbital pair breaking is usually negligible. For instance, in CeCu_2Si_2 and $\kappa\text{-(BEDT-TTF)}_2\text{Cu(NCS)}_2$, the Maki parameter α_M is ~ 10 [49] and ~ 8 [50], in which the T^*/T_c ratio is even close to 0.6. It has been

shown that orbital effects are detrimental to the formation of the FFLO state [4]; the FFLO region will shrink due to the orbital effect, leading to a lower critical temperature. For KFe_2As_2 , the Maki parameter is only ~ 3 , which is indeed much smaller than that of the heavy fermion and organic superconductors. Therefore, one possible explanation is that the orbital pair breaking cannot be ignored in KFe_2As_2 . We note that an upturn in $B_{c2}(T)$ also appears at a relatively low temperature ($T^* \approx 0.2T_c$) in FeSe [15], where α_M is found to be similar to KFe_2As_2 as ~ 5 (2.5) for the electron (hole) pocket. Therefore, it is possible that both compounds have a significant orbital pair breaking, resulting in the occurrence of low critical temperature T^* . Additionally, considering that KFe_2As_2 is the multiband superconductor, the band structure may also be a factor influencing the critical temperature T^* . The numerical calculations have shown that the electrons from the isotropic Fermi surface can strongly reduce the stability of the FFLO state and decreases its region in the phase diagram due to the quantum band geometric effects [38]. Indeed, the α and γ Fermi surfaces are nearly isotropic [33] in KFe_2As_2 , which might play a role.

Our result is different from the previous transport measurements [34] (see Fig. S9 [42]). Some comments are in order. Previous transport measurements suggested that the FFLO state appears below $T^* \approx 1.5$ K. However, our studies indicate that the FFLO state actually emerges at a lower temperature of $T^* \approx 0.8$ K even at $B \approx 5.3$ T, coinciding with an upturn in the upper critical field. The presence of impurities in the sample is known to influence the appearance of the FFLO state, typically resulting in its occurrence at lower temperatures with higher impurity levels. However, our sample exhibits a higher T_c than previously studied samples [34,42], which is an indication of fewer impurities. It is unlikely that this difference can be attributed to impurity effects. We believe that the discrepancy arises with the large uncertainty in determined T^* from the specific heat results [34]. Finally, it is worth noting that, while the T_c of previously studied samples was found to be lower than ours [34], the temperature dependence of the upper critical magnetic field at $B > 4$ T is consistent with our findings [42], suggesting that the observed FFLO state seems surprisingly robust against impurities. This behavior seems to contradict the presence of the FFLO state at high fields [9]. However, as already mentioned above, the isotropic superconducting gap on the α Fermi surface should contribute less to forming the FFLO state in KFe_2As_2 , while the anisotropic gaps on β and γ Fermi surfaces might play a more significant role. Previous research has suggested the presence of interstitial Fe in KFe_2As_2 [27,51], which serves as the magnetic impurity. Therefore, it is plausible that although

magnetic impurities affect the isotropic superconducting gap and result in reduced T_c at zero field, they may have minimal effect on the anisotropic superconducting gap and thus do not influence the presence of the FFLO state. For the fully opened gap with no sign-changing order parameter, the magnetic impurity is a pair breaker and breaks the time-reversal symmetry [52]. For the anisotropic superconducting gaps on β and γ Fermi surfaces, it is possible that the interband coupling makes them have more tolerance with magnetic impurities [53]. Further investigation is still required to study the impact of magnetic impurities on the FFLO state in KFe_2As_2 through the microscopic research on locally induced impurity states.

Summary. In summary, we have performed low-temperature and high-field ^{75}As -NMR measurements on the multiband iron-based superconductor KFe_2As_2 . A clear increase of the second moment of the spectrum, as well as a notable peak in the $1/T_1T$, are observed in the same low-temperature and high-field region, implying the emergence of superconducting spin smecticity and Andreev bound states due to the staggered distribution of normal and superconducting regions, which provides compelling microscopic evidence for the existence of the FFLO state. The obtained phase diagram reveals two unique characteristics: a distinct boundary line between the FFLO and HSC states and a low FFLO critical temperature $T^* \approx 0.2T_c$. These features can be attributed to the multiband effects. Our results offers new insights into the intrinsic properties and microscopic mechanisms underlying FFLO states.

Acknowledgments. We thank H. Adachi, T. Mizushima, and S. Kasahara for valuable discussions. This work was supported by National Key Research and Development Projects of China (Grants No. 2023YFA1406100 and No. 2022YFA1403402), the National Natural Science Foundation of China (Grants No. 12374142 and No. 12304170), Beijing National Laboratory for Condensed Matter Physics (Grant No. 2024BNLCMPKF005) and CAS PIFI program (2024PG0003). J.Z. and Z.K. were supported by the Key Program of the National Natural Science Foundation of China (Grant No. 12234006), the National Key R&D Program of China (Grant No. 2022YFA1403202), the Innovation Program for Quantum Science and Technology (Grant No. 2024ZD0300103), the Shanghai Municipal Science and Technology Major Project (Grant No. 2019SHZDZX01) and the Large Scientific Facility Open Subject of Songshan Lake Laboratory (Grant No. DG23313511). This work was supported by the Synergetic Extreme Condition User Facility (SECUF, [54]).

Data availability. The data supporting this study's findings are available within the Letter.

- [1] P. Fulde and R. A. Ferrell, Superconductivity in a strong spin-exchange field, *Phys. Rev.* **135**, A550 (1964).
- [2] A. I. Larkin and Y. N. Ovchinnikov, Nonuniform state of superconductors, *Sov. Phys. JETP* **20**, 762 (1964).
- [3] K. Maki and T. Tsuneto, Pauli paramagnetism and superconducting state, *Prog. Theor. Phys.* **31**, 945 (1964).

- [4] L. W. Gruenberg and L. Gunther, Fulde-Ferrell effect in type-II superconductors, *Phys. Rev. Lett.* **16**, 996 (1966).
- [5] G. Zwignagl and J. Wosnitzer, in *BCS: 50 Years*, edited by L. N. Cooper and D. Feldman (World Scientific, Singapore, 2011), pp. 337–371; G. Zwignagl and J. Wosnitzer, Breaking translational invariance by population imbalance: The

- Fulde-Ferrell-Larkin-Ovchinnikov states, *Int. J. Mod. Phys. B* **24**, 3915 (2010).
- [6] K. Maki, The magnetic properties of superconducting alloys. II, *Phys. Phys. Fiz.* **1**, 127 (1964).
- [7] S. Takada, Superconductivity in a molecular field. II: Stability of Fulde-Ferrel phase, *Prog. Theor. Phys.* **43**, 27 (1970).
- [8] Y. Matsuda and H. Shimahara, Fulde-Ferrell-Larkin-Ovchinnikov state in heavy Fermion superconductors, *J. Phys. Soc. Jpn.* **76**, 051005 (2007).
- [9] J. Wosnitzer, FFLO states in layered organic superconductors, *Ann. Phys. (NY)* **530**, 1700282 (2018).
- [10] S. Imajo, T. Kobayashi, A. Kawamoto, K. Kindo, and Y. Nakazawa, Thermodynamic evidence for the formation of a Fulde-Ferrell-Larkin-Ovchinnikov phase in the organic superconductor $\lambda - (\text{BETS})_2\text{GaCl}_4$, *Phys. Rev. B* **103**, L220501 (2021).
- [11] C. W. Cho, J. Lyu, C. Y. Ng, J. J. He, K. T. Lo, D. Chareev, T. A. Abdel-Baset, M. Abdel-Hafiez, and R. Lortz, Evidence for the Fulde-Ferrell-Larkin-Ovchinnikov state in bulk NbS_2 , *Nat. Commun.* **12**, 3676 (2021).
- [12] P. Wan, O. Zheliuk, N. F. Q. Yuan, X. Peng, L. Zhang, M. Liang, U. Zeitler, S. Wiedmann, N. E. Hussey, T. T. M. Palstra, T. M. Thomas, and J. Ye, Orbital Fulde-Ferrell-Larkin-Ovchinnikov state in an Ising superconductor, *Nature (London)* **619**, 46 (2023).
- [13] A. Ptok and D. Crivelli, The Fulde-Ferrell-Larkin-Ovchinnikov State in Pnictides, *J. Low Temp. Phys.* **172**, 226 (2013).
- [14] J. Paglione and R. L. Greene, High-temperature superconductivity in iron-based materials, *Nat. Phys.* **6**, 645 (2010).
- [15] S. Kasahara, Y. Sato, S. Licciardello, M. Čulo, S. Arsenijević, T. Ottenbros, T. Tominaga, J. Böker, I. Eremin, T. Shibauchi, J. Wosnitzer, N. E. Hussey, and Y. Matsuda, Evidence for an Fulde-Ferrell-Larkin-Ovchinnikov state with segmented vortices in the BCS-BEC-crossover superconductor FeSe , *Phys. Rev. Lett.* **124**, 107001 (2020).
- [16] S. Kasahara, H. Suzuki, T. Machida, Y. Sato, Y. Ukai, H. Murayama, S. Suetsugu, Y. Kasahara, T. Shibauchi, T. Hanaguri, and Y. Matsuda, Quasiparticle nodal plane in the Fulde-Ferrell-Larkin-Ovchinnikov state of FeSe , *Phys. Rev. Lett.* **127**, 257001 (2021).
- [17] N. Zhou, Y. Sun, C. Y. Xi, Z. S. Wang, J. L. Zhang, Y. Zhang, Y. F. Zhang, C. Q. Xu, Y. Q. Pan, J. J. Feng, Y. Meng, X. L. Yi, L. Pi, T. Tamegai, X. Xing, and Z. Shi, Disorder-robust high-field superconducting phase of FeSe single crystals, *Phys. Rev. B* **104**, L140504 (2021).
- [18] M. Ichioka, H. Adachi, T. Mizushima, and K. Machida, Vortex state in a Fulde-Ferrell-Larkin-Ovchinnikov superconductor based on quasiclassical theory, *Phys. Rev. B* **76**, 014503 (2007).
- [19] A. B. Vorontsov, J. A. Sauls, and M. J. Graf, Phase diagram and spectroscopy of Fulde-Ferrell-Larkin-Ovchinnikov states of two-dimensional d -wave superconductors, *Phys. Rev. B* **72**, 184501 (2005).
- [20] Y. Yanase and M. Sigrist, Antiferromagnetic order and π – Triplet pairing in the Fulde-Ferrell-Larkin-Ovchinnikov state, *J. Phys. Soc. Jpn.* **78**, 114715 (2009).
- [21] H. Mayaffre, S. Krämer, M. Horvatić, C. Berthier, K. Miyagawa, K. Kanoda, and V. F. Mitrović, Evidence of Andreev bound states as a hallmark of the FFLO phase in κ -(BEDT-TTF) $_2\text{Cu}(\text{NCS})_2$, *Nat. Phys.* **10**, 928 (2014).
- [22] A. Bianchi, R. Movshovich, N. Oeschler, P. Gegenwart, F. Steglich, J. D. Thompson, P. G. Pagliuso, and J. L. Sarrao, First-order superconducting phase transition in CeCoIn_5 , *Phys. Rev. Lett.* **89**, 137002 (2002).
- [23] K. Kumagai, M. Saitoh, T. Oyaizu, Y. Furukawa, S. Takashima, M. Nohara, H. Takagi, and Y. Matsuda, Fulde-Ferrell-Larkin-Ovchinnikov State in a Perpendicular Field of Quasi-Two-Dimensional CeCoIn_5 , *Phys. Rev. Lett.* **97**, 227002 (2006).
- [24] G. Koutroulakis, H. Kühne, J. A. Schlueter, J. Wosnitzer, and S. E. Brown, Microscopic study of the Fulde-Ferrell-Larkin-Ovchinnikov state in an all-organic superconductor, *Phys. Rev. Lett.* **116**, 067003 (2016).
- [25] K. Kinjo, M. Manago, S. Kitagawa, Z. Q. Mao, S. Yonezawa, Y. Maeno and K. Ishida, Superconducting spin smecticity evidencing the Fulde-Ferrell-Larkin-Ovchinnikov state in Sr_2RuO_4 , *Science* **376**, 397 (2022).
- [26] S. Kitagawa, G. Nakamine, K. Ishida, H. S. Jeevan, C. Geibel, and F. Steglich, Evidence for the presence of the Fulde-Ferrell-Larkin-Ovchinnikov state in CeCu_2Si_2 revealed using ^{63}Cu NMR, *Phys. Rev. Lett.* **121**, 157004 (2018).
- [27] Y. Liu, M. A. Tanatar, V. G. Kogan, H. Kim, T. A. Lograsso, and R. Prozorov, Upper critical field of high-quality single crystals of KFe_2As_2 , *Phys. Rev. B* **87**, 134513 (2013).
- [28] P. Burger, F. Hardy, D. Aoki, A. E. Böhrer, R. Eder, R. Heid, T. Wolf, P. Schweiss, R. Fromknecht, M. J. Jackson, C. Paulsen, and C. Meingast, Strong Pauli-limiting behavior of H_{c2} and uniaxial pressure dependencies in KFe_2As_2 , *Phys. Rev. B* **88**, 014517 (2013).
- [29] D. A. Zocco, K. Grube, F. Eilers, T. Wolf, and H. v. Löhneysen, Pauli-limited multiband superconductivity in KFe_2As_2 , *Phys. Rev. Lett.* **111**, 057007 (2013).
- [30] K. Okazaki, Y. Ota, Y. Kotani, W. Malaeb, Y. Ishida, T. Shimojima, T. Kiss, S. Watanabe, C.-T. Chen, K. Kihou, C. H. Lee, A. Iyo, H. Eisaki, T. Saito, H. Fukazawa, Y. Kohori, K. Hashimoto, T. Shibauchi, Y. Matsuda, H. Ikeda, H. Miyahara *et al.*, Octet-line node structure of superconducting order parameter in KFe_2As_2 , *Science* **337**, 1314 (2012).
- [31] T. Terashima, N. Kurita, M. Kimata, M. Tomita, S. Tsuchiya, M. Imai, A. Sato, K. Kihou, C. Lee, H. Kito, H. Eisaki, A. Iyo, T. Saito, H. Fukazawa, Y. Kohori, H. Harima, and S. Uji, Fermi surface in KFe_2As_2 determined via de Haas-van Alphen oscillation measurements, *Phys. Rev. B* **87**, 224512 (2013).
- [32] F. Hardy, A. E. Böhrer, D. Aoki, P. Burger, T. Wolf, P. Schweiss, R. Heid, P. Adelmann, Y. X. Yao, G. Kotliar, J. Schmalian, and C. Meingast, Evidence of strong correlations and coherence-incoherence crossover in the iron pnictide superconductor KFe_2As_2 , *Phys. Rev. Lett.* **111**, 027002 (2013).
- [33] D. Wu, J. Jia, J. Yang, W. Hong, Y. Shu, T. Miao, H. Yan, H. Rong, P. Ai, X. Zhang, C. Yin, J. Liu, H. Chen, Y. Yang, C. Peng, C. Li, S. Zhang, F. Zhang, F. Yang, Z. Wang, L. Zhao *et al.*, Nodal S_{\pm} pairing symmetry in an iron-based superconductor with only hole pockets, *Nat. Phys.* **20**, 571 (2024).
- [34] C.-W. Cho, J. H. Yang, N. F. Q. Yuan, J. Shen, T. Wolf, and R. Lortz, Thermodynamic evidence for the Fulde-Ferrell-Larkin-Ovchinnikov state in the KFe_2As_2 Superconductor, *Phys. Rev. Lett.* **119**, 217002 (2017).
- [35] A. Gurevich, Upper critical field and the Fulde-Ferrel-Larkin-Ovchinnikov transition in multiband superconductors, *Phys. Rev. B* **82**, 184504 (2010).

- [36] M. Takahashi, T. Mizushima, and K. Machida, Multiband effects on Fulde-Ferrell-Larkin-Ovchinnikov states of Pauli-limited superconductors, *Phys. Rev. B* **89**, 064505 (2014).
- [37] K. Adachi and R. Ikeda, Possible field-temperature phase diagrams of two-band superconductors with paramagnetic pair-breaking, *J. Phys. Soc. Jpn.* **84**, 064712 (2015).
- [38] T. Kitamura, A. Daido, and Y. Yanase, Quantum geometric effect on Fulde-Ferrell-Larkin-Ovchinnikov superconductivity, *Phys. Rev. B* **106**, 184507 (2022).
- [39] A. V. Chubukov, I. Eremin, and D. V. Efremov, Superconductivity versus bound-state formation in a two-band superconductor with small Fermi energy: Applications to Fe pnictides/chalcogenides and doped SrTiO₃, *Phys. Rev. B* **93**, 174516 (2016).
- [40] A. F. Wang, S. Y. Zhou, X. G. Luo, X. C. Hong, Y. J. Yan, J. J. Ying, P. Cheng, G. J. Ye, Z. J. Xiang, S. Y. Li, and X. H. Chen, Anomalous impurity effects in the iron-based superconductor KFe₂As₂, *Phys. Rev. B* **89**, 064510 (2014).
- [41] S. Shen, X. Zhang, H. Wo, Y. Shen, Y. Feng, A. Schneidewind, P. Čermákk, W. Wang, and J. Zhao, Neutron spin resonance in the heavily hole-doped KFe₂As₂ superconductor, *Phys. Rev. Lett.* **124**, 017001 (2020).
- [42] See Supplemental Material at <http://link.aps.org/supplemental/10.1103/7hhv-9fq7> for additional data and analysis.
- [43] A. Pustogow, Y. Luo, A. Chronister, Y.-S. Su, D. A. Sokolov, F. Jerzembeck, A. P. Mackenzie, C. W. Hicks, N. Kikugawa, S. Raghu, and E. D. Bauer, and S. E. Brown, Constraints on the superconducting order parameter in Sr₂RuO₄ from oxygen-17 nuclear magnetic resonance, *Nature (London)* **574**, 72 (2019).
- [44] B. M. Rosemeyer and A. B. Vorontsov, Spin susceptibility of Andreev bound states, *Phys. Rev. B* **94**, 144501 (2016).
- [45] T. Oka, Z. Li, S. Kawasaki, G. F. Chen, N. L. Wang, and G.-Q. Zheng, Antiferromagnetic spin fluctuations above the dome-shaped and full-gap superconducting states of LaFeAsO_{1-x}F_x revealed by ⁷⁵As-nuclear quadrupole resonance, *Phys. Rev. Lett.* **108**, 047001 (2012).
- [46] Z. Li, D. L. Sun, C. T. Lin, Y. H. Su, J. P. Hu, and G.-q. Zheng, Nodeless energy gaps of single-crystalline Ba_{0.68}K_{0.32}Fe₂As₂ as seen via ⁷⁵As NMR, *Phys. Rev. B* **83**, 140506(R) (2011).
- [47] P. S. Wang, P. Zhou, J. Dai, J. Zhang, X. X. Ding, H. Lin, H. H. Wen, B. Normand, R. Yu, and W. Yu, Nearly critical spin and charge fluctuations in KFe₂As₂ observed by high-pressure NMR, *Phys. Rev. B* **93**, 085129 (2016).
- [48] R. Beyer, B. Bergk, S. Yasin, J. A. Schlueter, and J. Wosnitza, Angle-dependent evolution of the Fulde-Ferrell-Larkin-Ovchinnikov state in an organic superconductor, *Phys. Rev. Lett.* **109**, 027003 (2012).
- [49] S. Kittaka, Y. Aoki, Y. Shimura, T. Sakakibara, S. Seiro, C. Geibel, F. Steglich, H. Ikeda, and K. Machida, Multiband superconductivity with unexpected deficiency of nodal quasiparticles in CeCu₂Si₂, *Phys. Rev. Lett.* **112**, 067002 (2014).
- [50] R. Lortz, Y. Wang, A. Demuer, P. H. M. Böttger, B. Bergk, G. Zwirgagl, Y. Nakazawa, and J. Wosnitza, Calorimetric evidence for a Fulde-Ferrell-Larkin-Ovchinnikov superconducting state in the layered organic superconductor κ-(BEDT-TTF)₂Cu(NCS)₂, *Phys. Rev. Lett.* **99**, 187002 (2007).
- [51] V. Grinenko, S.-L. Drechsler, M. Abdel-Hafez, S. Aswartham, A. U. B. Wolter, S. Wurmehl, C. Hess, K. Nenkov, G. Fuchs, D. V. Efremov, B. Holzapfel, J. van den Brink, and B. Büchner, Disordered magnetism in superconducting KFe₂As₂ single crystals, *Phys. Status Solidi B* **250**, 593 (2013).
- [52] P. W. Anderson, Theory of dirty superconductors., *J. Phys. Chem. Solids* **11**, 26 (1959).
- [53] J. Li and Y. Wang, Magnetic impurities in the two-band *s*_±-wave superconductors, *Europhys. Lett.* **88**, 17009 (2009).
- [54] <https://cstr.cn/31123.02.SECUF>.